International Journal of Nanomedicine

Dovepress
open access to scientific and medical research

Open Access Full Text Article

ORIGINAL RESEARCH

Nitroxide-Modified Protein-Incorporated Nanoflowers with Dual Enzyme-Like Activities

This article was published in the following Dove Press journal:
International Journal of Nanomedicine

Zhuofu Wu[1,2]
Sitong Zhang[1]
Xiaojun Wang[2]
Can Cai[2]
Guang Chen[1]
Li Ma[2]

[1]Key Laboratory of Straw Biology and Utilization, The Ministry of Education, College of Life Science, Jilin Agricultural University, Changchun 130118, People's Republic of China; [2]Department of Physics, Georgia Southern University, Statesboro, GA 30460, USA

Purpose: Combined superoxide dismutase (SOD)/catalase mimetics have attracted much attention because of their efficacy against reactive oxygen species-associated diseases; however, their application is often limited owing to their poor stability and the absence of favorable grafting sites. To address this, we developed a new class of SOD/catalase mimetics based on hybrid nanoflowers, which exhibit superior stability and possess the desired grafting sites for drugs and endogenous molecules.

Methods: In this work, for the first time, we used polynitroxylated human serum albumin (PNA) to mediate the formation of hybrid copper-based nanoflowers. H_2O_2 depletion and O_2 evolution assays were first performed to determine the catalase-like activity of the hybrid nanoflowers. Next, the xanthine oxidase/cytochrome c method was used to assay the SOD-like activity of the nanoflowers. Further characteristics of the nanoflowers were evaluated using scanning electron microscopy (SEM), electron paramagnetic resonance (EPR), and Fourier-transform infrared spectroscopy (FTIR). Operational stability was assessed via the reusability assay.

Results: The H_2O_2 depletion and O_2 evolution assays indicated that PNA-incorporated nanoflowers have genuine catalase-like activity. Kinetic analysis revealed that the reactions of the incorporated nanoflowers with H_2O_2 not only obey Michaelis–Menton kinetics, but that the nanoflowers also possess a higher affinity for H_2O_2 than that of native catalase. The FTIR spectra corroborated the presence of PNA in the hybrid nanoflowers, while the EPR spectra confirmed the intermolecular interaction of nitroxides bound to the human serum albumin incorporated into the nanoflowers. The remarkable operational reproducibility of the hybrid nanoflowers in catalase-like and SOD-like reactions was verified across successive batches.

Conclusion: Herein, a comparison of Michaelis constants showed that the hybrid nanoflower, a catalase mimetics, outperforms the native catalase. Acting as a "better-than-nature" enzyme mimetics, the hybrid nanoflower with superior stability and desired ligand grafting sites will find widespread utilization in the medical sciences.

Keywords: catalase, superoxide dismutase, polynitroxylated human serum albumin, reactive oxygen species, copper-based nanoflowers

Correspondence: Guang Chen
College of Life Science, Jilin Agricultural University, No. 2888 Xincheng Avenue, Changchun 130118, People's Republic of China
Tel/Fax +86 431 8453 2942
Email guangc61@gmail.com

Li Ma
Department of Physics, Georgia Southern University, 65 Georgia Avenue, Math/Physics Building Room 1003, Statesboro, GA 30460, USA
Tel +1 912 478 5950
Fax +1 912 478 0471
Email lma@GeorgiaSouthern.edu

Introduction

Acting as potential therapeutic agents, combined synthetic superoxide dismutase (SOD)/catalase mimetics can prevent oxidative stress in living organisms by removing the reactive oxygen species (ROS) that cause aging.[1,2] Many researchers in this field have focused on investigating salen–manganese (III) complexes, which possess superoxide and hydrogen peroxide scavenging properties that could counter ROS-associated diseases.[3,4] Although salen–manganese (III) complexes exhibit better bioavailability and enzymatic behavior than antioxidant enzymes, the stability of these complexes can be significantly reduced under oxidizing conditions owing to ligand degradation.[5]

submit your manuscript | www.dovepress.com
DovePress
http://doi.org/10.2147/IJN.S220718

In recent years, a number of nanomaterials possessing SOD and catalase activities have attracted much attention, such as nanoceria, Mn3O4, and platinum nanoparticles.[6–8] To be used as therapeutic agents for additional applications, such as for targeted drug delivery, affinity ligands must be grafted to the surface of SOD/catalase mimetics using nanostructures.[9] Because the majority of the reactions of SOD/catalase mimetics with nanostructures occur on the surface of these nanomaterials, surface grafting causes a significant decrease in the dual enzyme-like activities of mimetics.[10] Hence, this remains a critical challenge in constructing combined synthetic SOD/catalase mimetics that possess sufficient grafting sites and perfect stability.

It is generally accepted that amino acid side chains in proteins can provide enough grafting sites for affinity ligands. Hence, we propose that biomolecule-inspired synthesis would be a suitable approach for introducing protein into the nanostructure of mimetics with SOD and catalase activities, overcoming problems arising from surface grafting. In a previous report, protein-incorporated nanoflowers were fabricated using a molecular assembly of protein and copper phosphor.[11] The protein molecules serve as "glue" to bind the petals together during the growth of the nanoflowers, which consequently expending into mature $Cu_3(PO_4)_2$ nanoflowers. It is thought that the grafting sites for the required ligands are supplied by the amino acid side chains of the protein which are incorporated into the nanoflowers; these hybrid nanoflowers are regarded as mimetics possessing dual enzyme activities. Moreover, hybrid nanoflowers have been shown to exhibit excellent operational stability in the resolution of (*R, S*)-2-pentanol.[12] The skeletal stability of $Cu_3(PO_4)_2$ hybrid nanoflowers permits their reuse within medical and industrial fields.

It has been confirmed that hybrid nanoflowers exert a peroxidase-like activity that relies on a Fenton-like reaction mechanism.[13] Might it be possible to endow them with a catalase-like activity using this ingenious approach? In a prior study, nitroxide radicals were used to stimulate the catalase mimetic activity of the heme protein.[14] The mechanism of stimulation was attributed to the replenishment of MbFe III and to the detoxification of MbFe IV, which was accelerated by nitroxide radicals that can "shuttle" among three oxidation states. Inspired by this work, we surmised that, if nitroxide radical molecules had been incorporated into the nanoflowers, then these radicals should accelerate the conversion of copper (II) ions to copper (I) ions in the nanoflowers by shuttling among their different oxidation states, facilitating H_2O_2 disproportionation. Specifically, the catalase mimetic activity of the nanoflowers should be activated by the nitroxide radicals incorporated into the nanoflowers. Furthermore, although nitroxides have SOD-like activity, their utilization is limited owing to their short half-life in vivo.[15] Fortunately, the half-life and SOD-like activity of nitroxides can be improved by covalent attachment to the backbone of protein.[16,17]

On the basis of the above-mentioned reports, we speculated that human serum albumin decorated by nitroxides is the perfect candidate to mediate the formation of nanoflowers with SOD and catalase mimetic activities. We hypothesized that the nitroxides would stimulate the catalase mimetic activity of copper ions in the nanoflowers in the manner of inducing the corresponding activity of MbFe III in the heme protein. Furthermore, we predicted that the amino acid groups of the human serum albumin would provide sufficient grafting sites for the affinity ligands to avoid the capping of copper ions on the surface of the nanoflower, and that nitroxide covalently attached to human serum albumin incorporated into the nanoflowers would still maintain its initial SOD-like activity.

In this study, polynitroxylated human serum albumin (PNA) was employed to direct the synthesis of the hybrid nanoflowers (Scheme 1). The material characteristics of the nanoflowers were assessed using SEM, FTIR and EPR. The catalase mimetic activity and corresponding kinetic parameters of nanoflowers were determined using the H_2O_2 depletion and O_2 evolution assays. The SOD-like activity of the nanoflowers was determined by the xanthine oxidase/cytochrome c method. Finally, the reusability of the hybrid nanoflowers was assessed via the H_2O_2 depletion assay and the xanthine oxidase/cytochrome c method.

Materials and Methods

Reagent and Materials

The following reagents were purchased from Sigma-Aldrich Chemical Co. (St. Louis, MO, USA): nitroxide 2,2,6,6-tetramethylpiperdine 1-oxyl (Tempo), human serum albumin (HSA); catalase (from bovine liver; 2000–5000 units/mg protein; one unit decomposes hydrogen peroxide at a rate of 1.0 μmol/min at pH 7.0 at 25°C; in 1 min, the hydrogen peroxide concentration falls from 10.3 mM to 9.2 mM); bovine superoxide dismutase (≥2500 units/mg protein; one unit inhibits the rate of reduction of cytochrome c by 50% in a coupled system using xanthine and xanthine oxidase at pH

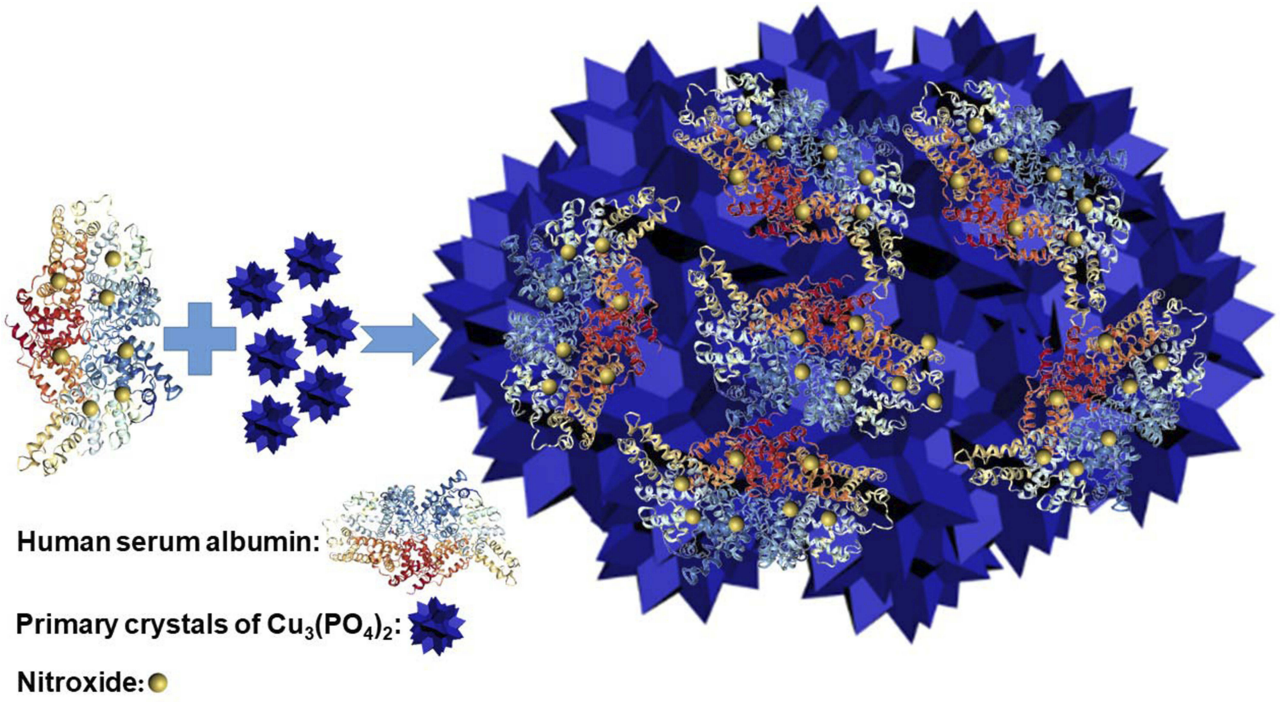

Scheme 1 Synthesis of polynitroxylated human serum albumin-incorporated nanoflowers.

7.8 at 25°C in a 3.0 mL reaction volume; the xanthine oxidase concentration used causes a change in absorbance of 0.025 min-1 at 550 nm); xanthine oxidase (from bovine milk; ≥0.4 units/mg protein; one unit converts xanthine to uric acid at a rate of 1.0 µmol/min at pH 7.5 at 25°C); cytochrome c (≥95%, SDS-PAGE); and acetaldehyde (≥99.0%, GC). All chemicals and reagents were of analytical grade. All aqueous solutions were prepared with Milli-Q water purification system (Millipore, Bedford, MA, USA).

Synthesis of the Hybrid Nanoflowers

PNA was prepared according to a previously published method,[15,18–20] with a nitroxide/albumin molar ratio of 50:1. Synthesis of the hybrid nanoflowers was performed according to the classical method, with necessary modifications.[11] PNA (150 mg/mL) was diluted to 0.02, 0.05, 0.10, and 0.50 mg/mL concentrations in PBS buffer (0.05 M, pH 7.4). The synthesis was started by adding 20 mL $CuSO_4$ solution (120 mM) to 3 L of the PBS buffer containing PNA. After incubation at 25°C for 3 d, the precipitate was separated from the mixture by centrifugation (10 min, 8000 g, 25°C). The precipitate was washed with deionized water 3 times and then dried. The final product was termed the "PNA-incorporated nanoflowers". To calculate the production yield, the residual protein content in the supernatant was determined by the Bradford method,[21] using bovine serum albumin as a standard. The encapsulation yield of fixed PNA was calculated by the difference between the amounts of PNA used and the amounts recovered in the supernatant. All samples were measured by EPR spectroscopy, and the amount of nitroxides per gram of flowers in each sample was calculated by double integrating the EPR spectrum against a standard curve. The standard curve was constructed by spiking a test solution with multiple known amounts of Tempo. The encapsulation yields were 100%, 97%, 70%, and 18% for the samples prepared using 0.02, 0.05, 0.10, and 0.50 mg/mL PNA, respectively, which is consistent with the results from the EPR data. The hybrid nanoflowers obtained which were prepared from 0.02, 0.05, 0.10, and 0.50 mg/mL PNA were termed PNA-nano-A, PNA-nano-B, PNA-nano-C, and PNA-nano-D, respectively. For the control group, HSA solutions of differing concentrations in PBS in the range of 0.02–0.50 mg/mL were also used to synthesize HSA-incorporated nanoflowers (which are referred to by this name hereafter).

Characterization of Hybrid Nanoflowers

The morphologies of the samples were surveyed using a scanning electron microscope (JEOL JSM-7600F, JEOL Ltd., Tokyo, Japan) operated at 25 kV. The FTIR absorption spectra of samples were taken over a 400–4000 cm^{-1} range using a Thermo iS10 FTIR (Thermo Fisher Scientific,

Waltham, MA, USA) (×2) with a resolution of 4 cm^{-1}. EPR spectra were recorded using an X-band EPR spectrometer (Bruker EMXplus, Bruker Instruments, Inc., Berlin, Germany). Spectroscopic data collection parameters were as follows: center field, 3340 G; scan range, 200 G; field modulation, 0.79 G; microwave power, 0.5 mW; time constant, 0.1 s.

Assessment of H_2O_2

The decomposition of H_2O_2 by the hybrid nanoflowers was measured on the basis of the spectrophotometric method.[22] The hybrid nanoflowers (10 mg) were suspended in 100 mL of deionized water (0.1 mg/mL) and allowed to stand for 5 min. The decomposition reaction of H_2O_2 was triggered by the addition of 150 μL hybrid nanoflower mixture to 9 mL H_2O_2 (12 mM) during magnetic stirring. The reaction mixture was incubated at 25°C for 3 min. An aliquot of the reaction mixture (1 mL) was withdrawn every 30 s and then filtrated by a membrane filter (0.22 μm pore size). The absorbance decrease of the filtrate at 240 nm (ε = 43.6 $M^{-1}cm^{-1}$) was monitored using an Agilent 8453 UV-VIS spectrophotometer (Agilent Technologies, Santa Clara, CA, USA) to determine the residual amount of H_2O_2. The specific activity (μmol min^{-1} mg^{-1}) was defined as the amount of H_2O_2 decomposed per minute per milligram of the hybrid nanoflowers.

Evaluation of O_2 Evolution

The conversion of hydrogen peroxide to oxygen was monitored using the Clark-type oxygen electrode method.[23] The hybrid nanoflower mixture (0.10 mg/mL) prepared above was further diluted by 10 times with deionized water. The reaction mixture consisted of 3 mL H_2O_2 (12 mM) and 50 μL diluted hybrid nanoflower mixture (0.01 mg/mL). The reaction was initiated after adding the diluted nanoflowers. The oxygen concentration was monitored for 180 s at 25°C using a 5300A biological oxygen monitor (YSI Incorporated, Yellow Springs, OH, USA).

Kinetic Parameters

The Michaelis–Menten constants K_m and V_{max} for the catalase-like activity of the hybrid nanoflowers were determined by measuring the initial rates at different H_2O_2 concentrations ranging from 3 to 60 mM with different concentrations of nanoflowers. After obtaining the initial rate versus H_2O_2 concentration data, the values of Vmax and Km were derived using a Lineweaver–Burk plot.[24] Turnover numbers (k_{cat}) of the hybrid nanoflowers were calculated according to the equation:

$$K_{cat} = V_{max}/[E]$$

where [E] is the amount of PNA or HSA incorporated into the nanoflowers in the reaction mixture. Catalytic efficiencies (k_{cat}/K_m) of the hybrid nanoflowers were also calculated.

SOD-Like Activity Assay

The method of inhibition of cytochrome c reduction in the acetaldehyde/xanthine oxidase system was employed to evaluate the SOD-like activity of superoxide dismutase and the hybrid nanoflowers.[25] The reaction system of superoxide generation contained 300 μL cytochrome c (0.5 mg/mL), 20 μL acetaldehyde (100 mM), and 0.3 μL xanthine oxidase (11.2 U/mL). The inhibition reaction of cytochrome c reduction was trigged by adding 30 μL superoxide dismutase (0.1 mg/mL) or 30 μL PNA-incorporated nanoflowers (1.2 mg/mL). The reaction system was incubated at 25°C for 15 min. The absorbance increase of the reaction system at 550 nm was monitored with an Agilent 8453 UV-VIS spectrophotometer. For the PNA-incorporated nanoflowers, 330 μL solutions identical to those used to produce the superoxide were prepared. After adding the PNA-incorporated nanoflowers, each of the above-mentioned solutions was centrifuged at an interval of 3 min from each other and then the absorbance of the supernatant was recorded. The reduction rate of cytochrome c was calculated by the slope of the curve within the initial 3 min. One unit of SOD is defined as the amount of enzyme required to inhibit the reduction rate of cytochrome c by 50% under the above-mentioned conditions.

Reusability

The repeated batch decomposition of 12 mM H_2O_2 by the hybrid nanoflowers was performed at 25°C for 3 min. At the end of each batch, the hybrid nanoflowers were separated from the reaction mixture by centrifugation (8000 rpm, 3 min) and washed with distilled water to remove any residual substrate or product. After each round of centrifugation, the nitroxide signal of the suspension was detected using an EPR spectrometer. Then, the recycled hybrid nanoflowers were incubated in a vacuum oven overnight for drying. The dried powder was employed again for the subsequent reaction cycle. The residual activity of the recycled catalase mimetic was compared with the initial catalase-like activity of the first cycle (100%). The SOD-like activities of the

hybrid nanoflowers before and after 10 cycles were also determined according to the above-mentioned assay.

Statistical Analysis

The data obtained from the various experiments were plotted using Origin 8.5 and expressed as the mean ± standard error. Each value represents the mean of data from three independent experiments performed in duplicate, with an average standard deviation <5%.

Results and Discussion

Dismutation of H_2O_2 and Evolution of O_2

To investigate the effect of the amount of PNA on the catalase mimetic activity of the PNA-incorporated nanoflowers, they were prepared at different PNA concentrations ranging from 0.02 to 0.50 mg/mL. As can be seen in Figure 1, the concentration of hydrogen peroxide in the reaction solution continued to decrease with the extension of the reaction time. Accordingly, as shown in Figure 2, the concentration of oxygen continuously increased with accumulating reaction time. It is worth noting that the rate of H_2O_2 decay was about two times higher than the rate of O2 evolution for every sample, which provides direct evidence of the genuine catalase-like activity of nanoflowers.[26] In the H_2O_2 depletion and O_2 evolution assays, PNA-nano-B demonstrated the optimal decay rate of H_2O_2 and evolution rate of O_2 compared with the other samples.

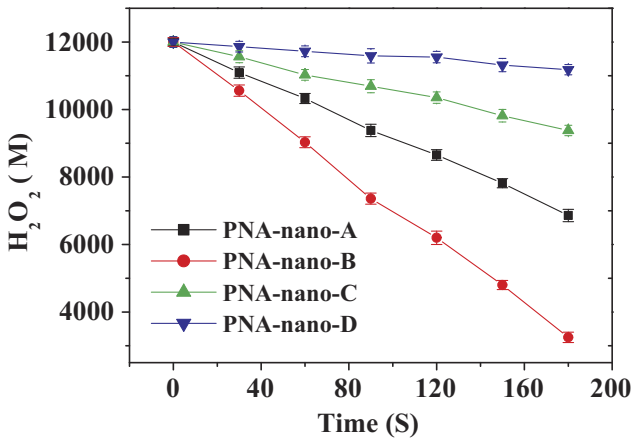

Figure 1 H_2O_2 depletion catalyzed by PNA-incorporated nanoflowers.

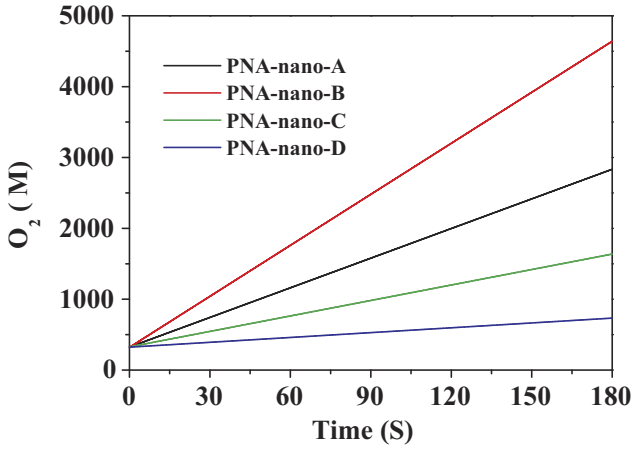

Figure 2 O_2 evolution catalyzed by PNA-incorporated nanoflowers.

Table 1 The Specific Activity of the PNA-Incorporated Nanoflowers

Nanoflower	Specific Activity (μmol/min/mg)
PNA-nano-A	1004.02 ± 34.32
PNA-nano-B	1782.03 ± 37.60
PNA-nano-C	584.01 ± 29.88
PNA-nano-D	164.00 ± 32.45

The specific activities of the hybrid nanoflowers were calculated according to the rate of H_2O_2 decay during the initial 1 min of the reaction time and are listed in Table 1. The results supported the conclusion that PNA-nano-B possesses the optimal specific activity (1782.03 ± 37.60 μmol min^{-1} mg^{-1}). Hence, PNA-nano-B was used for the subsequent experiments. In comparison with PNA-nano-A, PNA-nano-B showed a 1.77-fold increase in the specific activity. The results show that increasing the concentration of PNA used encourages an enhanced amount of nitroxide to bind to the HSA incorporated into the nanoflowers (Figure 3). Therefore, the 1.77-fold enhancement in the specific activity of PNA-nano-B should be attributed to the increase in the amount of nitroxide

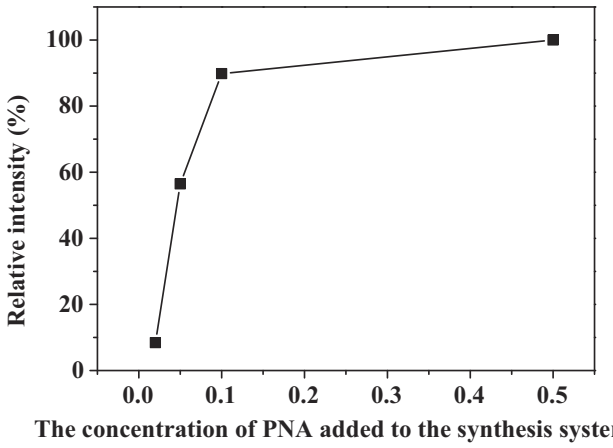

Figure 3 The effect of PNA on the amount of nitroxide encapsulated into the nanoflowers.

bound to HSA incorporated into the nanoflowers. Moreover, PNA-nano-B showed 3.05-fold and 10.87-fold increases compared with PNA-nano-C and PNA-nano-D, respectively. The SEM images show that PNA-nano-A and PNA-nano-B possess excellent branched, flower-like morphologies with a size of 4–10 μM (Figure 4A–H). In contrast, PNA-nano-C and PNA-nano-D nanoflowers have lost their hierarchical structure, which plays an essential role in the mass transfer diffusion of substrate and of product in the enzymatic reaction (Figure 4I–P). For PNA-nano-C and PNA-nano-D, the mass transfer limitation of the substrate and product caused by the loss of hierarchical structure leads to a poor specific activity. From this, it can be deduced that the catalase mimetic activity of the PNA-incorporated nanoflowers depends on the amount of nitroxide bound to PNA incorporated into the nanoflowers and their hierarchical structures. For the corresponding sample without PNA, no nanoflowers could be obtained (see Figure S1) and there was no measurable catalase-like activity.

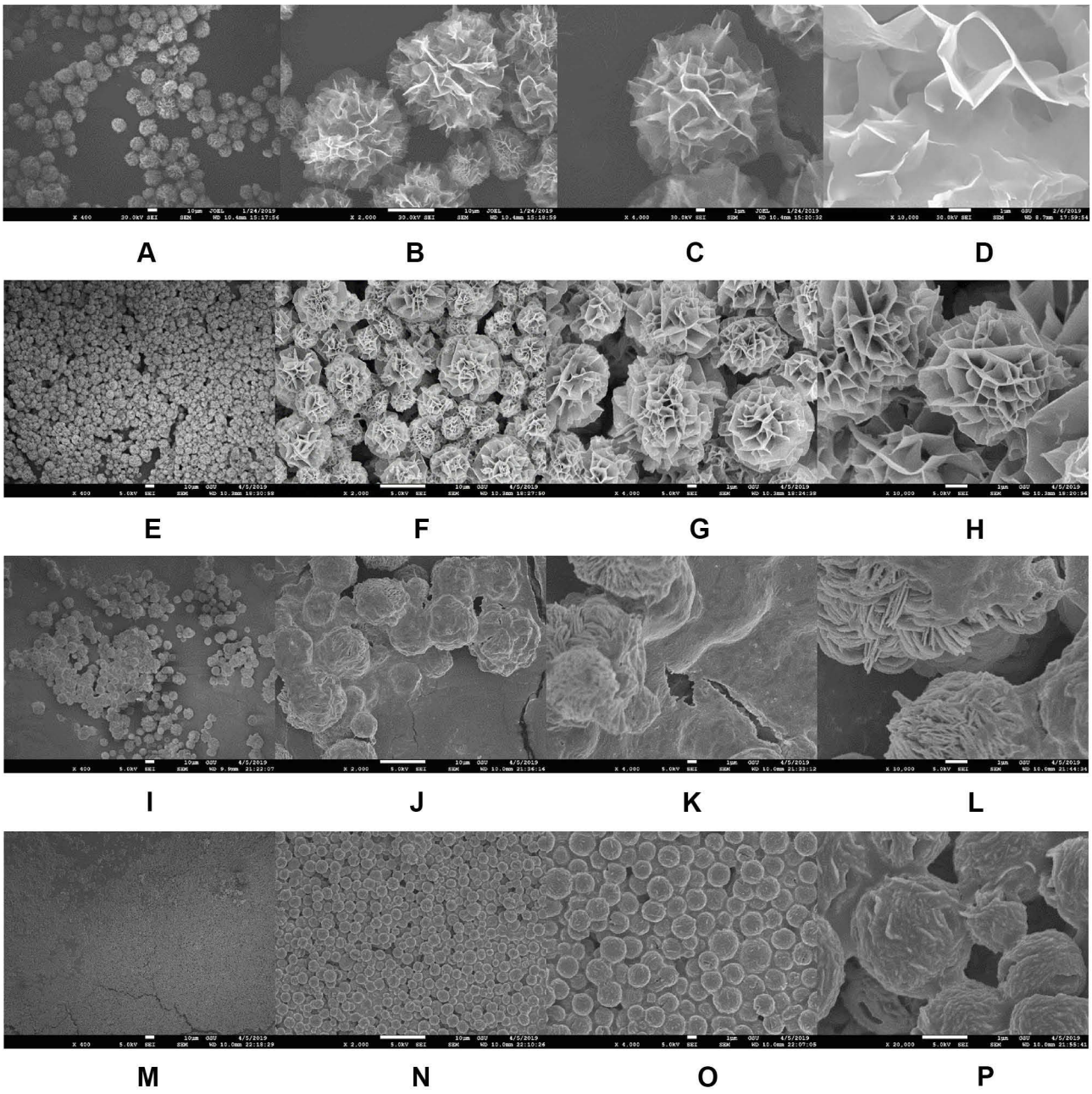

Figure 4 SEM images of the PNA-nano-A (**A**–**D**), PNA-nano-B (**E**–**H**), PNA-nano-C (**I**–**L**), and PNA-nano-D (**M**–**P**) samples.

FTIR Spectra

As shown by curve (a) in Figure 5, the presence of the $Cu_3(PO_4)_2$ component was confirmed by the characteristic $PO4^{3-}$ bands at 1053 cm^{-1} and 556 cm^{-1}.[27] The existence of PNA was verified by the amide I and II bands of the protein at 1651 cm^{-1} and 1542 cm^{-1} in curve (c) of Figure 5.[28] In curve (b) of Figure 5, the presence of both the characteristic $PO4^{3-}$ bands and the amide I and II protein bands proves that PNA is present in the $Cu_3(PO_4)_2$ nanoflowers.

EPR Spectra

From Figure 6, it can be observed that the nanoflowers show characteristic nitroxide peaks in a magnetic field range of 3320–3360 G. In comparison with soluble PNA, a widening of the peak-valley (I, II, III) was observed for PNA-incorporated nanoflowers, which can be ascribed to the intermolecular interaction of nitroxides bound to the HSA incorporated into the nanoflowers.

Kinetic Analysis

The kinetics of the catalase-like activity of the PNA-incorporated nanoflowers was further analyzed based on apparent steady-state kinetics. The initial reaction velocities were calculated from the slopes of the H_2O_2 depletion and O_2 evolution assays. As shown in Figures 7 and 8, as the concentration of PNA incorporated into nanoflowers remains constant, the velocities of H_2O_2 depletion and O_2 evolution gradually approach plateau, accompanying the rising H_2O_2 concentration; this conforms to the enzymatic characteristics

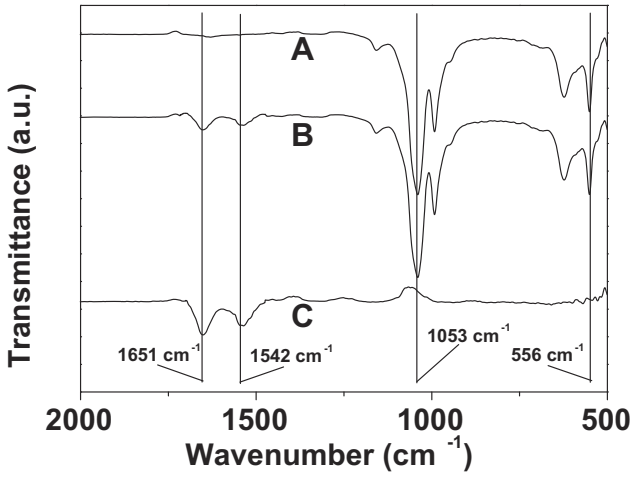

Figure 5 FTIR spectra of $Cu_3(PO_4)_2$ crystal without PNA (**A**), the PNA-incorporated nanoflowers (**B**), and PNA (**C**).

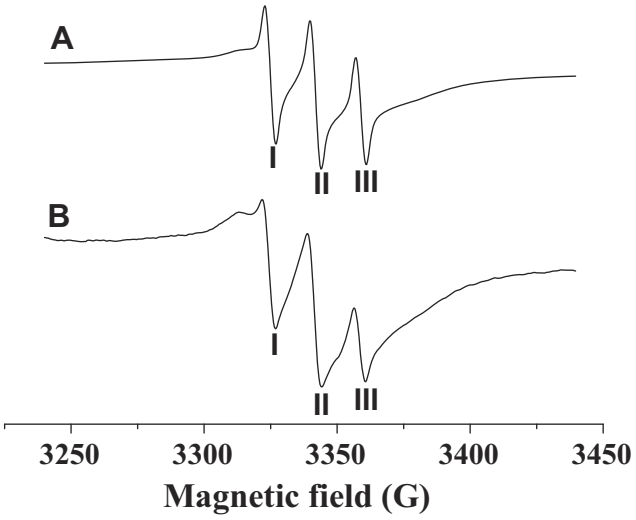

Figure 6 EPR spectra of PNA (**A**) and PNA-incorporated nanoflowers (**B**).

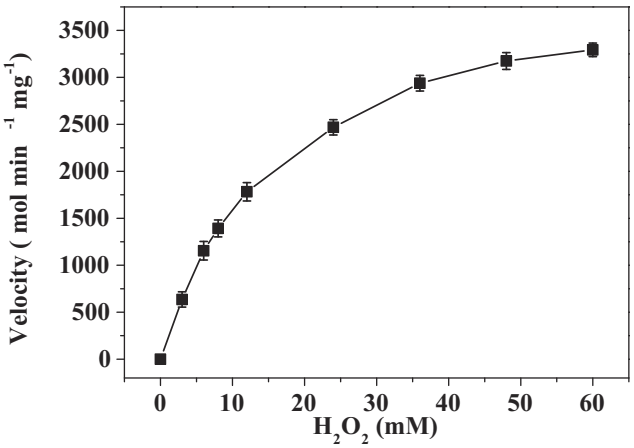

Figure 7 Steady-state kinetic assay of the PNA-incorporated nanoflowers. Velocity indicates the rate of H_2O_2 depletion.

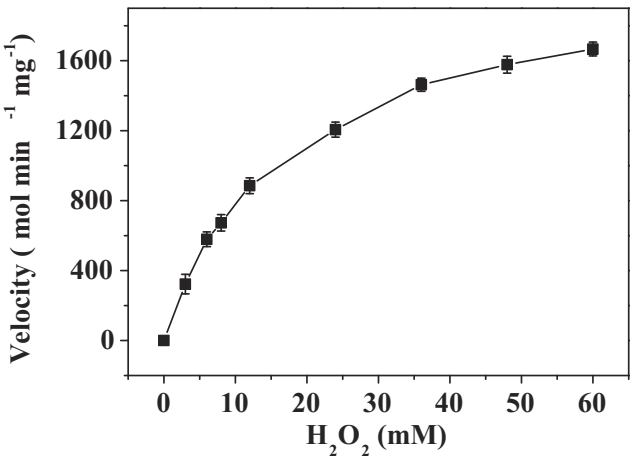

Figure 8 Steady-state kinetic assay of the PNA-incorporated nanoflowers. Velocity indicates the rate of O_2 evolution.

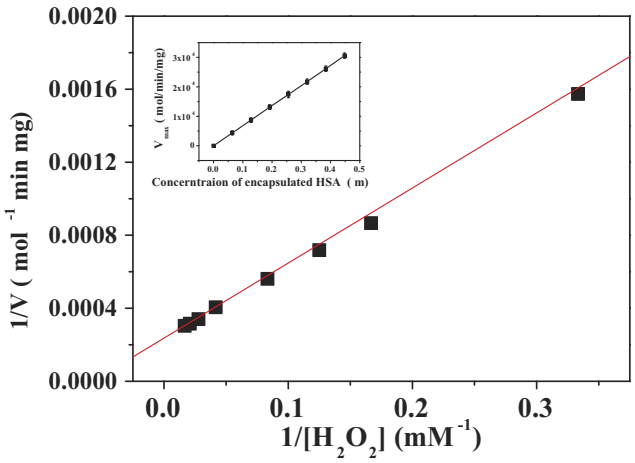

Figure 9 Lineweaver–Burk plots of the reaction velocity of the PNA-incorporated nanoflowers as a function of H_2O_2 concentration ranging from 3 to 60 mM. V indicates the rate of H_2O_2 depletion.

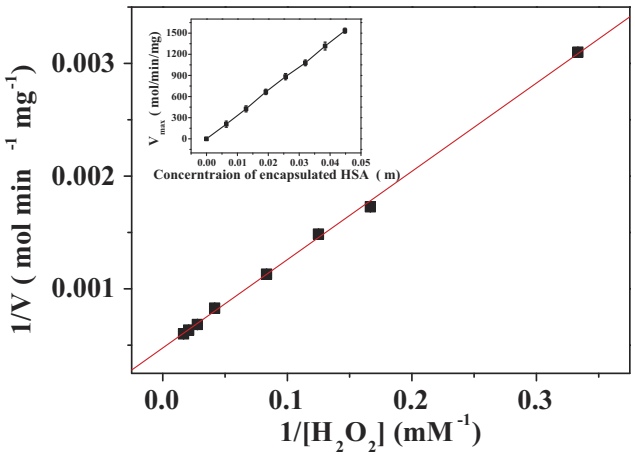

Figure 10 Lineweaver–Burk plots of the reaction velocity of the PNA-incorporated nanoflowers as a function of H_2O_2 concentration ranging from 3 to 60 mM. V indicates the rate of O_2 evolution.

of native catalase.[25] On the Lineweaver–Burk double reciprocal plot, a good linear relationship can be observed between V^{-1} and $[S]^{-1}$ (Figure 9 and Figure 10). The K_m and V_{max} values of the PNA-incorporated nanoflowers were calculated using the slope and intercept of the line in Figure 9 and are shown in Table 2. From Table 2, the K_m value of the native catalase is 1.64 times higher than that of the PNA-incorporated nanoflowers. This suggests that the PNA-incorporated nanoflowers have a 1.64-fold increase in affinity for H_2O_2 compared with that of the native catalase. The increased affinity can be ascribed to the presence of more active sites on the surface of the PNA-incorporated nanoflowers compared with the native catalase which has four active sites per enzyme molecule.[30] However, the V_{max}, K_{cat} (S^{-1}), and K_{cat}/K_m ($M^{-1}S^{-1}$) of the native catalase are 32.50, 15.89, and 10.00 times higher than those of PNA-incorporated nanoflowers, respectively. The lower V_{max}, K_{cat} (S^{-1}), and K_{cat}/K_m ($M^{-1}S^{-1}$) of the nanoflowers may be due to two reasons: (i) PNA-incorporated nanoflowers lack the shape and properties of the heme distal pocket of the native catalase;[31] and (ii) the ratio of Cu ions in the nanoflowers to nitroxide bound to HSA incorporated into the nanoflowers is relatively low, meaning that some Cu ions in the nanoflowers cannot be stimulated by nitroxide.

Because the absorbance of catalase at 280 nm would be expected to interfere with H_2O_2 detection, the O_2 evolution assay was performed to compare the activity of native catalase, PNA-incorporated nanoflowers, and HSA-incorporated nanoflowers. The results showed that PNA-incorporated nanoflowers exhibit 5.21% catalytic activity relative to the native catalase, and that PNA-incorporated nanoflowers show a 32.3-fold increase in catalase-like activity compared with that of the HSA-incorporated nanoflowers (Figure 11). It has been reported that the nitroxide catalase-like activity in the presence of heme iron relies on the cyclical conversion of ferryl hemoglobin/methemoglobin.[14] In the current experiment, a distinct difference in the catalase-like activity of the hybrid nanoflowers could be observed in the presence or absence of nitroxides. Hence, we speculated that the close proximity of nitroxide to the Cu ion in the nanoflowers potentially accelerates the oxidative/reductive cycle occurring between Cu II and Cu I (Figure 12), which creates genuine catalase-like activity in the nanoflowers. Moreover, the experimental data show that the activity of native superoxide dismutase is 3.37 times higher than that of soluble nitroxide (2,2,6,6-tetramethylpiperidine 1-oxyl) and that the SOD-like activity of the nitroxide encapsulated into the hybrid nanoflowers is the same as that of the soluble nitroxide.

Table 2 Comparison of Kinetic Parameters Between PNA-Incorporated Nanoflowers and Native Catalase

Catalysts	K_m (mM)	V_{max} (μmol/min/mg)	K_{cat} (S^{-1})	K_{cat}/K_m ($M^{-1}S^{-1}$)
PNA-incorporated nanoflowers	17.41	0.44×10^4	3.78×10^4	0.21×10^7
Catalase from bovine liver[29]	28.60	1.43×10^5	60.06×10^4	2.10×10^7

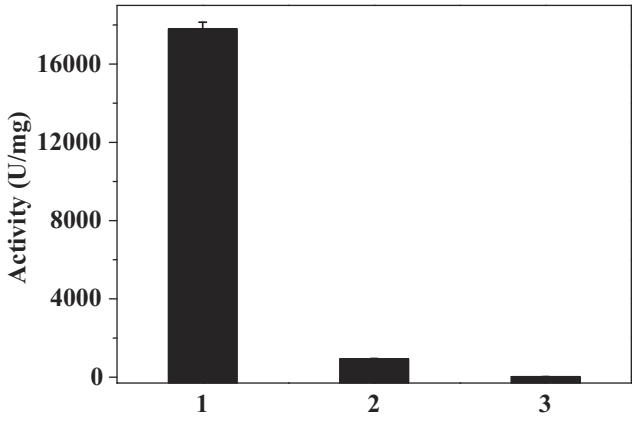

Figure 11 O_2 evolution catalyzed by native catalase (1), PNA-incorporated nanoflowers (2), and HSA-incorporated nanoflowers (3). For each reaction condition, the amounts of sample used for the assay were: 10 μL native catalase (0.001 mg/mL), 50 μL PNA-incorporated nanoflowers (0.01 mg/mL), and 50 μL HSA-incorporated nanoflowers (0.01 mg/mL). One unit of activity is defined as the evolution of 1 μmol/min of oxygen at 25°C in deionized water.

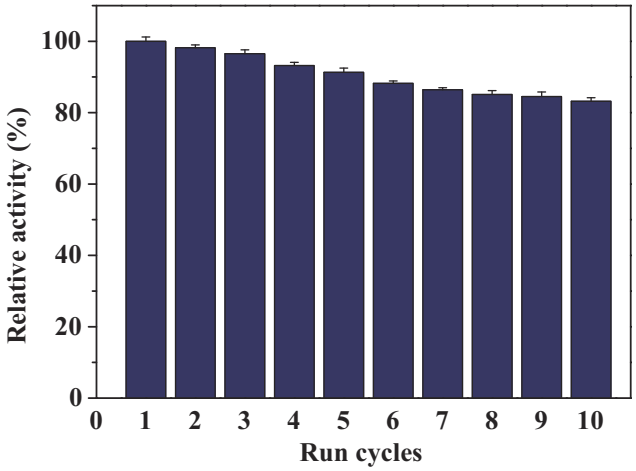

Figure 13 Reuse of PNA-incorporated nanoflowers.

Reusability of Hybrid Nanoflowers

The reusability of the PNA-incorporated nanoflowers was studied across 10 continuous runs to evaluate their value for practical applications. The results indicate that the PNA-incorporated nanoflowers maintain 83.3% of their initial catalase mimetic activity after 10 cycles (Figure 13), which is consistent with the change in the intensity of nitroxide bound to the HSA incorporated into the nanoflowers on an EPR spectrum (See Figure S2). In addition, no absorption related to protein or nitroxide could be detected in the supernatant collected from the reaction system at the end of each run. This implies that, during the reaction, PNA does not escape from the nanoflower matrix, and that there is no decomposition of the nitroxide from the HSA. Hence, the 16.7% decrease in catalase mimetic activity during the continuous runs is due to the loss of the PNA-incorporated nanoflowers caused by repeated washing. Moreover, after 10 cycles, the nanoflowers still retained 83.5% of their initial SOD-like activity (see Figure S3). The decrease of SOD-like activity should therefore be attributed to the loss of nanoflowers during continuous operational use. The excellent reusability of PNA-incorporated nanoflowers implies that they have the potential to be industrially amplified for use in removing ROS and in preventing oxidative stress in clinical applications. The excellent performance of hybrid nanoflowers in mimicking catalase and SOD sets the stage for a cascade of radical scavenging reactions. It can be further speculated that the hybrid nanoflowers could act as a prospectively useful tool for controlling oxidative stress, similar to the antioxidant properties of other nanomaterials, which have been already been investigated in existing studies.[32–37]

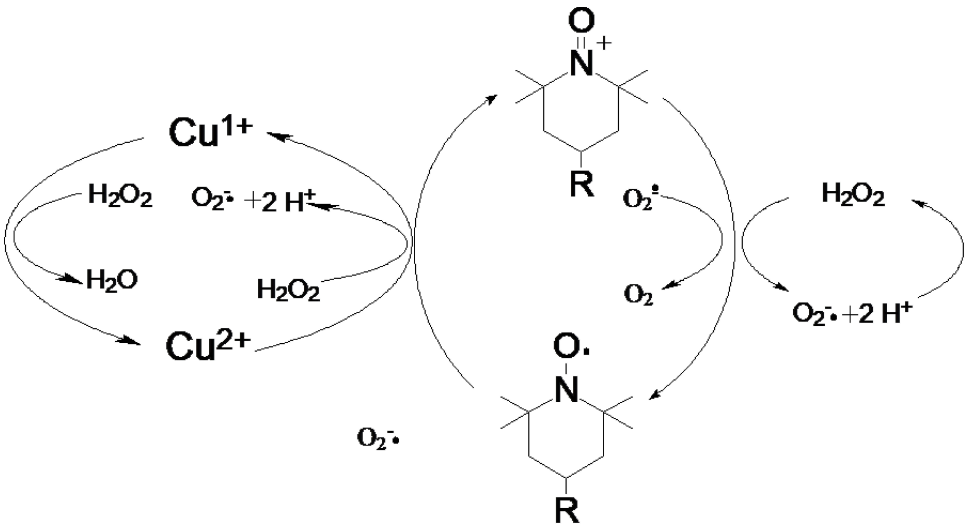

Figure 12 The catalytic mechanism of PNA-incorporated nanoflowers with dual enzyme-like activities.

Conclusion

In this study, PNA-incorporated nanoflowers with catalase and superoxide dismutase-like activities were fabricated based on inspiration from nitroxide-modified HSA. The PNA-incorporated nanoflowers not only showed a higher affinity for H_2O_2 than that of the native catalase, but further, in catalase-like and superoxide dismutase-like reactions, exhibited perfect reusability across 10 continuous cycles. Thus, this endows the nanoflowers with the potential to treat diseases associated with ROS. Provided that HSA in the hybrid nanoflowers can be replaced by or covalently linked to other enzymes commonly used in medical diagnostics, the applications to which PNA-incorporated nanoflowers with dual enzyme-like activities can be applied can be greatly expanded. Furthermore, the reactive functional groups (thiol, amino, and carboxyl) offered by the protein encapsulated into the nanoflowers can be employed to bind many drugs and endogenous molecules. This makes these nanoflowers a promising carrier system for drug delivery. These promising, potential features of PNA-incorporated nanoflowers should allow us to further exploit their applications in the medical sciences.

Acknowledgments

This work was supported financially by the Key Laboratory of Straw Biology and Utilization Foundation of China (2019(39)) and China Scholarship Council (CSC, File No. 201808220076).

Author Contributions

All authors contributed to data analysis, drafting or revising the article, gave final approval of the version to be published, and agree to be accountable for all aspects of the work.

Disclosure

The authors report no conflicts of interest in this work.

References

1. Rong Y, Doctrow SR, Tocco G, Baudry M. EUK-134, a synthetic superoxide dismutase and catalase mimetic, prevents oxidative stress and attenuates kainate-induced neuropathology. *Proc Natl Acad Sci*. 1999;96(17):9897–9902. doi:10.1073/pnas.96.17.9897
2. Melov S, Ravenscroft J, Malik S, et al. Extension of life-span with superoxide dismutase/catalase mimetics. *Science*. 2000;289(5484):1567–1569. doi:10.1126/science.289.5484.1567
3. Baker K, Marcus CB, Huffman K, Kruk H, Malfroy B, Doctrow SR. Synthetic combined superoxide dismutase/catalase mimetics are protective as a delayed treatment in a rat stroke model: a key role for reactive oxygen species in ischemic brain injury. *J Pharmacol Exp Ther*. 1998;284(1):215–221.
4. Jung C, Rong Y, Doctrow S, Baudry M, Malfroy B, Xu Z. Synthetic superoxide dismutase/catalase mimetics reduce oxidative stress and prolong survival in a mouse amyotrophic lateral sclerosis model. *Neurosci Lett*. 2001;304(3):157–160. doi:10.1016/S0304-3940(01)01784-0
5. Baleizao C, Garcia H. Chiral salen complexes: an overview to recoverable and reusable homogeneous and heterogeneous catalysts. *Chem Rev*. 2006;106(9):3987–4043. doi:10.1021/cr050973n
6. Pirmohamed T, Dowding JM, Singh S, et al. Nanoceria exhibit redox state-dependent catalase mimetic activity. *Chem Commun*. 2010;46(16):2736–2738. doi:10.1039/B922024K
7. Singh N, Savanur MA, Srivastava S, D'Silva P, Mugesh G. A redox modulatory Mn3O4 nanozyme with multi-enzyme activity provides efficient cytoprotection to human cells in a parkinson's disease model. *Angew Chem Int Ed*. 2017;56(45):14267–14271. doi:10.1002/anie.201708573
8. Kajita M, Hikosaka K, Iitsuka M, Kanayama A, Toshima N, Miyamoto Y. Platinum nanoparticle is a useful scavenger of superoxide anion and hydrogen peroxide. *Free Radical Res*. 2007;41(6):615–626. doi:10.1080/10715760601169679
9. Sapsford KE, Algar WR, Berti L, et al. Functionalizing nanoparticles with biological molecules: developing chemistries that facilitate nanotechnology. *Chem Rev*. 2013;113(3):1904–2074. doi:10.1021/cr300143v
10. Zhou Y, Liu B, Yang R, Liu J. Filling in the gaps between nanozymes and enzymes: challenges and opportunities. *Bioconjugate Chem*. 2017;28(12):2903–2909. doi:10.1021/acs.bioconjchem.7b00673
11. Ge J, Lei J, Zare RN. Protein-inorganic hybrid nanoflowers. *Nat Nanotechnol*. 2012;7(7):428–432. doi:10.1038/nnano.2012.80
12. Wu Z, Li X, Li F, et al. Enantioselective transesterification of (R, S)-2-pentanol catalyzed by a new flower-like nanobioreactor. *RSC Adv*. 2014;4(64):33998–34002. doi:10.1039/C4RA04431B
13. Wu Z-F, Wang Z, Zhang Y, et al. Amino acids-incorporated nanoflowers with an intrinsic peroxidase-like activity. *Sci Rep*. 2016;6:22412. doi:10.1038/srep22412
14. Krishna MC, Samuni A, Taira J, Goldstein S, Mitchell JB, Russo A. Stimulation by nitroxides of catalase-like activity of hemeproteins kinetics and mechanism. *J Biol Chem*. 1996;271(42):26018–26025. doi:10.1074/jbc.271.42.26018
15. Kuppusamy P, Wang P, Zweier JL, et al. Electron paramagnetic resonance imaging of rat heart with nitroxide and polynitroxyl-albumin. *Biochemistry*. 1996;35(22):7051–7057. doi:10.1021/bi952857s
16. Li H, Ma L, Hsia CJ, Zweier JL, Kuppusamy P. Polynitroxyl-albumin (PNA) enhances myocardial infarction therapeutic effect of tempol in rat hearts subjected to regional ischemia-reperfusion. *Free Radical Biol Med*. 2002;32(8):712–719. doi:10.1016/S0891-5849(02)00762-1
17. Zhang S, Li H, Ma L, et al. Polynitroxyl-albumin (PNA) plus tempol attenuate lung capillary leak elicited by prolonged intestinal ischemia and reperfusion. *Free Radical Biol Med*. 2000;29(1):42–50. doi:10.1016/S0891-5849(00)00295-1
18. Ma L, Wang X-J. Characteristic emission in glutaraldehyde polymerized hemoglobin. *J Lumin*. 2011;131(3):461–464. doi:10.1016/j.jlumin.2010.10.029
19. Cao S, Zhang J, Ma L, Hsia CJ, Koehler RC. Transfusion of polynitroxylated pegylated hemoglobin stabilizes pial arterial dilation and decreases infarct volume after transient middle cerebral artery occlusion. *J Am Heart Assoc*. 2017;6(9):e006505. doi:10.1161/JAHA.117.006505
20. Hsia CJC, Ma L. A hemoglobin-based multifunctional therapeutic: polynitroxylated pegylated hemoglobin. *Artif Organs*. 2012;36(2):215–220. doi:10.1111/aor.2012.36.issue-2
21. Bradford MM. A rapid and sensitive method for the quantitation of microgram quantities of protein utilizing the principle of protein-dye binding. *Anal Biochem*. 1976;72(1):248–254. doi:10.1016/0003-2697(76)90527-3
22. Lartillot S, Kedziora P, Athias A. Purification and characterization of a new fungal catalase. *Prep Biochem*. 1988;18(3):241–246. doi:10.1080/00327488808062526

23. Escobar L, Salvador C, Contreras M, Escamilla JE. On the application of the Clark oxygen electrode to the study of enzyme kinetics in apolar solvents: the catalase reaction. *Anal Biochem*. 1990;184(1):139–144. doi:10.1016/0003-2697(90)90026-6
24. Lineweaver H, Burk D. The determination of enzyme dissociation constants. *J Am Chem Soc*. 1934;56(3):658–666. doi:10.1021/ja01318a036
25. Trnka J, Blaikie FH, Logan A, Smith RAJ, Murphy MP. Antioxidant properties of MitoTEMPOL and its hydroxylamine. *Free Radical Res*. 2009;43(1):4–12. doi:10.1080/10715760802582183
26. Stadtman E, Berlett B, Chock P. Manganese-dependent disproportionation of hydrogen peroxide in bicarbonate buffer. *Proc Natl Acad Sci*. 1990;87(1):384–388. doi:10.1073/pnas.87.1.384
27. Cho IS, Kim DW, Lee S, et al. Synthesis of Cu2PO4OH hierarchical superstructures with photocatalytic activity in visible light. *Adv Funct Mater*. 2008;18(15):2154–2162. doi:10.1002/adfm.200800167
28. Yang W-J, Griffiths PR, Byler DM, Susi H. Protein conformation by infrared spectroscopy: resolution enhancement by Fourier self-deconvolution. *Appl Spectrosc*. 1985;39(2):282–287. doi:10.1366/0003702854248917
29. Tukel SS, Alptekin O. Immobilization and kinetics of catalase onto magnesium silicate. *Process Biochem*. 2004;39(12):2149–2155. doi:10.1016/j.procbio.2003.11.010
30. Murthy MRN, Reid TJ, Sicignano A, Tanaka N, Rossmann MG. Structure of beef liver catalase. *J Mol Biol*. 1981;152(2):465–499. doi:10.1016/0022-2836(81)90254-0
31. Fita I, Rossmann MG. The active center of catalase. *J Mol Biol*. 1985;185(1):21–37. doi:10.1016/0022-2836(85)90180-9
32. Neupane BP, Chaudhary D, Paudel S, et al. Himalayan honey loaded iron oxide nanoparticles: synthesis, characterization and study of antioxidant and antimicrobial activities. *Int J Nanomed*. 2019;14:3533. doi:10.2147/IJN.S196671
33. Yang M, Zhang M, Nakajima H, Yudasaka M, Iijima S, Okazaki T. Time-dependent degradation of carbon nanotubes correlates with decreased reactive oxygen species generation in macrophages. *Int J Nanomed*. 2019;14:2797. doi:10.2147/IJN.S199187
34. Khorrami MB, Sadeghnia HR, Pasdar A, et al. antioxidant and toxicity studies of biosynthesized cerium oxide nanoparticles in rats. *Int J Nanomed*. 2019;14:2915. doi:10.2147/IJN.S194192
35. Xu C, Qiao L, Ma L, et al. Biogenic selenium nanoparticles synthesized by Lactobacillus casei ATCC 393 alleviate intestinal epithelial barrier dysfunction caused by oxidative stress via Nrf2 signaling-mediated mitochondrial pathway. *Int J Nanomed*. 2019;14:4491–4502. doi:10.2147/IJN.S199193
36. Wen T, Yang A, Piao L, et al. Comparative study of in vitro effects of different nanoparticles at non-cytotoxic concentration on the adherens junction of human vascular endothelial cells. *Int J Nanomed*. 2019;14:4475–4489. doi:10.2147/IJN.S208225
37. Pei Y, Cui F, Du X, et al. Antioxidative nanofullerol inhibits macrophage activation and development of osteoarthritis in rats. *Int J Nanomed*. 2019;14:4145–4155. doi:10.2147/IJN.S202466